PHYSICAL REVIEW A **77**, 033417 (2008)

Optical pumping by a laser pulse traveling in a cavity

Takuya Majima,[1] Akira Terasaki,[2] and Tamotsu Kondow[2]
[1]*East Tokyo Laboratory, Genesis Research Institute, Inc., 717-86 Futamata, Ichikawa, Chiba 272-0001, Japan*
[2]*Cluster Research Laboratory, Toyota Technological Institute in East Tokyo Laboratory, Genesis Research Institute, Inc., 717-86 Futamata, Ichikawa, Chiba 272-0001, Japan*
(Received 28 November 2007; published 24 March 2008)

We have developed a general method to perform optical pumping by a pulsed laser with the aid of an optical cavity (cavity-assisted optical pumping). Optical pumping is achieved by repetitive interaction of a single laser pulse with a target material in the cavity. This method is demonstrated for manganese ions, Mn^+, stored in a linear radio-frequency ion trap; about 10^8 ions are spin polarized by a 5-ns laser pulse via $^7P_J \leftarrow {}^7S_3$ ($J=3$ or 4) transition in the ultraviolet region. The linewidth of the pulsed light source is broad enough to transfer the populations of lower hyperfine levels to the highest one ($F=11/2$) in the $^7S_3$ ground state; the nuclear spin is polarized as well.

DOI: 10.1103/PhysRevA.77.033417 PACS number(s): 32.80.Xx, 32.10.Fn, 37.10.Ty, 37.20.+j

Optical pumping [1] is a powerful technique for spin polarization widely used since the first idea of Kastler in 1950 [2]. It is operated by repeated cycles of absorption of circularly polarized light and spontaneous emission back to the initial state. This cycle transfers angular momentum of photons to target atoms. The atoms eventually reach a nonstatistical population distribution, where only one of the magnetic sublevels is populated. Spin-polarized atoms and nuclei thus produced have a variety of applications [3–5]: Highly precise spectroscopy especially with double resonance techniques [6,7], spin-exchange collisions [8], manipulation and state-control of atoms [9], sensitive magnetometry [10], and so forth.

Although the advent of tunable lasers greatly expanded the application of optical pumping, the light source has been limited to continuous-wave (cw) lasers. This is due to the long interaction time needed to repeat the pumping cycles until the spin-polarization process is completed; the time scale is typically longer than several microseconds. Therefore, standard nanosecond laser pulses are not suitable for the light source. Recently, several schemes have been proposed for pulsed lasers to generate spin-polarized atomic ions without relying on optical pumping [11]. The elaborate schemes, however, have been applied only to alkaline-earth elements; the ground-state atoms in $^1S_0$ are excited by a circularly polarized laser pulse to $^3P_1$ ($M_J=+1$), and further ionization results in spin-polarized ions in the $^2S_{1/2}$ ground state. The advantage of pulsed lasers over cw ones, particularly in the tunability in short wavelengths, urges us to develop a new method with broader applicability.

In this paper, we present "cavity-assisted optical pumping," which allows us to perform optical pumping by a laser pulse with the aid of an optical cavity. It is shown that repeated interaction of a single laser pulse produces high-degree spin polarization of target materials in the cavity. This method provides a general technique for using pulsed lasers in a manner similar to cw light sources. The broad linewidth inherent to pulsed lasers enables nuclear spins to be polarized as well by exciting transitions split by hyperfine structures.

In the experiment, we have created a spin-polarized ensemble of about 10^8 ions of manganese, Mn^+, stored in a linear ion trap. Mn^+ has a nuclear and an electron spin of $I=5/2$ and $J=3$, respectively, in the ground state ($^7S_3$) with an electronic configuration of $3d^54s^1$. We have observed spin polarization of Mn^+ ions in the highest angular momentum of $F=J+I=11/2$; the ions are forced to populate in the sublevel of the magnetic quantum number $M=+11/2$ by interaction with a laser pulse of σ^+ circular polarization.

Figure 1 shows a schematic diagram of the experiment. Manganese ions were produced by a magnetron-sputter ion source, transferred by ion-beam guides and deflectors, and introduced into a 40-cm linear octopole ion trap, as described in detail elsewhere [12]. About 2×10^8 ions were loaded in 0.3 s and thermalized with buffer He gas at room temperature for 1.0 s. The ion trap was placed in a high-finesse optical cavity with a cavity length, $d=1.6$ m; the reflectivity, R, of the mirrors was 99.98% in the vicinity of 260 nm, where $^7P_J \leftarrow {}^7S_3$ ($J=2$, 3, and 4) transitions of Mn^+ are located [13–15]. A weak magnetic field (5 mT) was applied to the ion trap by a solenoidal magnet parallel to the laser beam in order to define the quantization axis. The stored ions interacted with a circularly polarized laser pulse (σ^+ polariza-

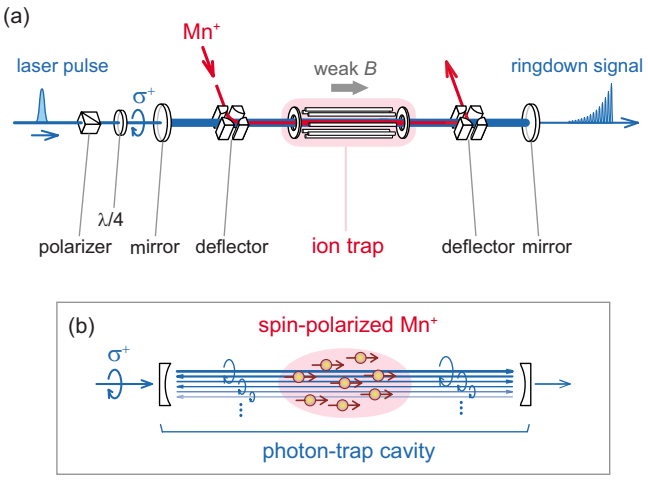

FIG. 1. (Color online) (a) A schematic diagram of the experimental setup. λ/4 is a quarter-wave plate for generating σ^+ polarization. (b) An illustration of spin polarization.

tion) with a duration of about 5 ns from a frequency-doubled output of an optical parametric oscillator (MOPO-HF +FDO, Spectra Physics) operated at 10 Hz. The experiment was performed for two different pulse energies: 0.2 mJ and 2 μJ as measured in front of the entrance mirror outside the cavity.

The optical cavity plays two roles in the present experiment: (1) It elongates the duration of the short laser pulse to excite the ions repetitively for optical pumping. (2) It provides a method for monitoring spin polarization through high-sensitivity measurements of optical absorption; spin polarization causes a change in absorbance because the transition probabilities depend on the magnetic sublevels populated.

Role (1) is essential for optical pumping by a laser pulse. The high-finesse cavity provides a lifetime of the incident laser pulse of 26.67 μs $(=d/[c(1-R)]$; c, the velocity of light); that is, the cavity stretches the 5-ns laser pulse by a factor of more than 5000 in duration. The laser pulse travels in the cavity during the lifetime and interacts with the trapped ions repeatedly. The selection rule of $\Delta M=+1$ holds even for the light propagating backward after reflection at the exit mirror, because the helicity of the light is reversed as well upon reflection [16,17]. Consequently, the optical pumping continues to proceed during the lifetime of the laser pulse.

Role (2) is important in evaluation of the degree of spin polarization subsequently to the optical pumping process. An absorbance of the ions in the trap is measured with the same laser pulse by the procedure of cavity ring-down spectroscopy [18] (or photon-trap spectroscopy for generality [12,19,20]). The technique measures the decay-rate constant (a reciprocal of the storage lifetime) of the laser pulse in the cavity for high-sensitivity absorption spectroscopy; the difference in the rate constants obtained for a filled and an empty ion trap provides an absorbance due to the ions. In an actual measurement, the temporal profile of the signal pulse leaking out from the exit mirror is fitted to an exponential function in the time range either between 10 and 60 μs (for weak absorption) or between 1 and 10 μs (for strong absorption). Spin polarization occurred prior to the fitting time range is evidenced by increase or decrease in the absorbance thus measured.

Experimental results are shown in Fig. 2 for $^7P_J \leftarrow {}^7S_3$ ($J=3$ and 4) transitions. They exhibit entirely different spectral profiles depending on the pulse energy. The data obtained by a 2-μJ laser pulse show ordinary absorption spectra split by hyperfine structures [Figs. 2(b) and 2(d)], which are identical to those observed by linearly polarized light [12]. These results imply that the pulse energy is not sufficiently high to cause a population imbalance among magnetic sublevels. Both the spectra are well fitted by incorporating all the hyperfine components weighted by their transition strengths. The fitting curves were obtained by representing each transition line by two Gaussian profiles with the full-width at half-maximum of 0.13 and 1.3 cm^{-1} with their intensity ratio of 1:0.15, which reproduced the spectral wing extending over 1 cm^{-1}; the wing structure was observed commonly in the present measurements probably because of the kinetic-energy distribution of the ions in the trap [12].

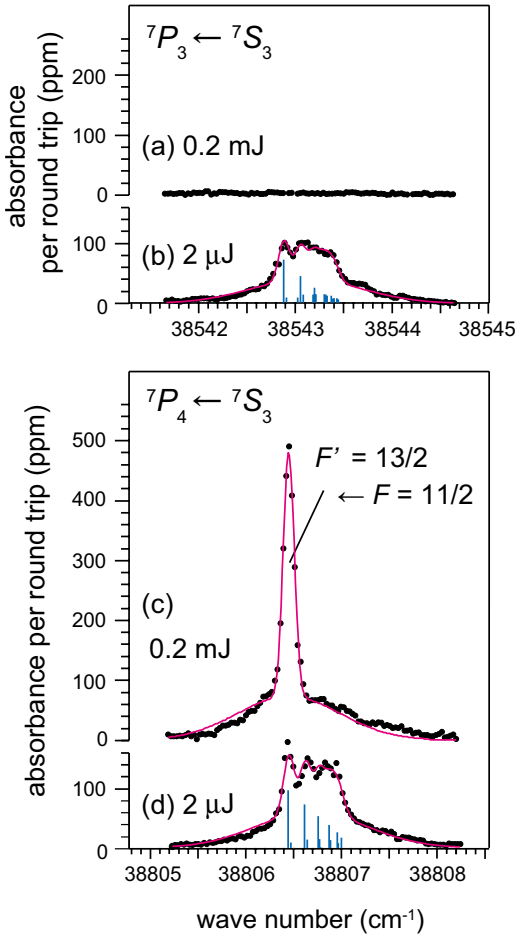

FIG. 2. (Color online) Optical absorption spectra of Mn^+ observed with σ^+-polarization laser pulses for (a,b) $^7P_3 \leftarrow {}^7S_3$ and (c,d) $^7P_4 \leftarrow {}^7S_3$ transitions. The pulse energy of the incident laser is either (a,c) 0.2 mJ or (b,d) 2 μJ. Solid circles are experimental data. Solid lines show fitting curves (see text for details). Bars indicate wave numbers of absorption lines; the length represents a relative intensity in the condition without spin polarization.

The spectral profiles change dramatically at a higher pulse energy of 0.2 mJ. Absorption peaks disappear completely in the spectrum of the $^7P_3 \leftarrow {}^7S_3$ transition [Fig. 2(a)] on the one hand; a single hyperfine component is enhanced in that of $^7P_4 \leftarrow {}^7S_3$ [Fig. 2(c)] on the other hand. The strong peak in the latter is assigned to a single absorption line of $F'=13/2 \leftarrow F=11/2$ with other ones bleached [see Fig. 3(a)], because the spectrum has a symmetrical profile and is reproduced well by the same double-Gaussian profile mentioned above including the wing structure.

These remarkable changes in the spectra depending on the pulse energy are due to (1) spin polarization in each F level and (2) population transfer from the lower to the highest F level. We first focus on the result for the high pulse-energy excitation of the $^7P_4 \leftarrow {}^7S_3$ transition [Fig. 2(c)]. The level scheme is shown in Fig. 3. When the laser frequency is tuned at the $F'=13/2 \leftarrow F=11/2$ transition, repeated excitation by the σ^+ polarization creates spin polarization to the $M=+11/2$ sublevel by the optical pumping process illustrated in Fig. 3(b). At the same time, due to the inherently

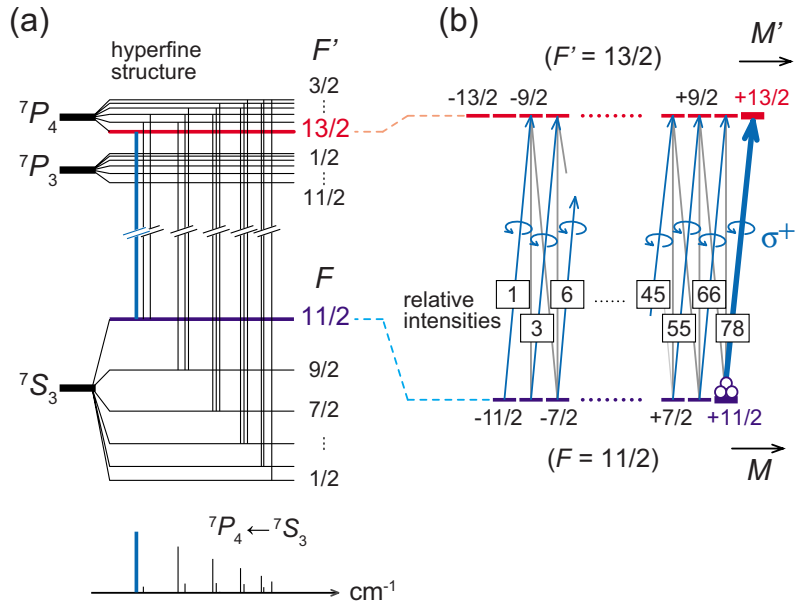

FIG. 3. (Color online) (a) The hyperfine energy diagram of $^7S_3$ and ^7P_J ($J=3$ and 4) states. (b) An illustration of the optical pumping process for the σ^+ transitions between sublevels of $F=11/2$ and those of $F'=13/2$; relative absorption intensities are indicated for each sublevel transition. $F(M)$ and F' (M') denote angular-momentum (magnetic) quantum numbers in the ground and the excited states, respectively.

broad spectral width of the laser pulse, ions in lower F levels ($F \leq 9/2$) are excited as well; spin polarization to the $M=+F$ sublevel is produced in each F level and the populations are promoted further to higher F levels through the excited state. Consequently, the optical absorption ends up with the single transition from $|F=11/2, M=+11/2\rangle$ to $|F'=13/2, M'=+13/2\rangle$. These processes take place also when the laser frequency is tuned at other hyperfine transitions; hence the absorption lines of the lower levels ($F \leq 9/2$) are bleached. Thus the single transition, $F'=13/2 \leftarrow F=11/2$, dominates the absorption spectrum with an enhanced intensity.

In the $^7P_3 \leftarrow {}^7S_3$ transition, on the other hand, the same argument holds for the $F \leq 9/2$ levels, whereas absorption is inhibited after spin polarization to the $|F=11/2, M=+11/2\rangle$ sublevel because of the absence of a $|F'=13/2, M'=+13/2\rangle$ sublevel in the $^7P_3$ excited state. This explains the complete disappearance of absorption in Fig. 2(a).

The enhancement factor of the $F'=13/2 \leftarrow F=11/2$ transition observed in the spectra of the $^7P_4 \leftarrow {}^7S_3$ absorption is analyzed as follows: The integrated absorption cross section shows that the transition observed at 0.2 mJ [Fig. 2(c)] is enhanced by a factor of 4.5 ± 0.5 compared with that observed at 2 μJ [Fig. 2(d)]. The primary cause of this enhancement is the increase in the transition probability due to spin polarization in the $F=11/2$ level; the relative intensity, $p(M)$, of σ^+ transition is given by $p(M) \propto (F+M+1)(F+M+2)/2$, as illustrated in Fig. 3(b) [21]. As a result of spin polarization to the $M=+11/2$ sublevel from an equally populated condition of all the sublevels, the transition probability increases by a factor of 2.6 $[=(2F+1)p(M=+11/2)/\Sigma_{M=-F}^{+F} p(M)]$. However, this factor alone cannot explain the experimental result.

The residual factor of the enhancement, $(4.5 \pm 0.5)/2.6$ $(\simeq 1.7 \pm 0.2)$, is ascribable to the secondary cause; the population of the $F=11/2$ level increases by the population transfer from the lower F levels. The initial population in the $F=11/2$ level in the $^7S_3$ ground state is 29% $[=(2F+1)/\Sigma_{F''=1/2}^{11/2}(2F''+1)]$ by assuming equally populated sublevels. Therefore, the factor of 1.7 ± 0.2 indicates that $49\% \pm 6\%$ of the stored ions are accumulated in the $|F=11/2, M=+11/2\rangle$ sublevel. This estimation of the degree of spin polarization places a lower bound, because the absorbance of the enhanced $F'=13/2 \leftarrow F=11/2$ transition is likely to be underestimated in the present measurement [22].

Finally, we show numerical simulations of the present optical pumping process to confirm the role of the cavity and to examine the pulse-energy dependence. For simplicity, the process between the two hyperfine levels, $F'=13/2$ and $F=11/2$, was simulated by solving rate equations for populations of relevant 26 $[=(2F'+1)+(2F+1)]$ magnetic sublevels [Fig. 3(b)]. It is known that the rate-equation scheme well describes the evolution of populations in the two-level system for time scales much longer than the natural lifetime of the excited state [23–25]; 3.61 and 3.68 ns for $^7P_3$ and $^7P_4$, respectively [14]. The parameters for the simulation were adjusted as follows: The initial pulse energy was set to be $\eta(1-R)E$, where E is the pulse energy (either 0.2 mJ or 2 μJ) measured prior to entrance to the cavity and η is the coupling efficiency of the incident laser beam to the cavity modes; η was fixed at unity. The pulse energy in the cavity was adjusted to decrease exponentially with time, according to the lifetime of the laser pulse; the lifetime was fixed at 10 μs by assuming a typical absorbance of the ions. The optical absorption rates immediately after the pulse injection were $(13\ \text{ns})^{-1}$ and $(1.3\ \mu\text{s})^{-1}$ for $E=0.2$ mJ and 2 μJ, respectively. Spin relaxation due to ion-ion and ion-buffer gas collisions was negligible, because the mean collision interval (>100 μs) was estimated to be longer than the time scale of the measurements.

The results of the simulations are shown in Fig. 4. Spin polarization in $M=+11/2$ and $M'=+13/2$ sublevels is achieved at about 1 μs after injection of a laser pulse with $E=0.2$ mJ [Fig. 4(a)]. This result shows that the original

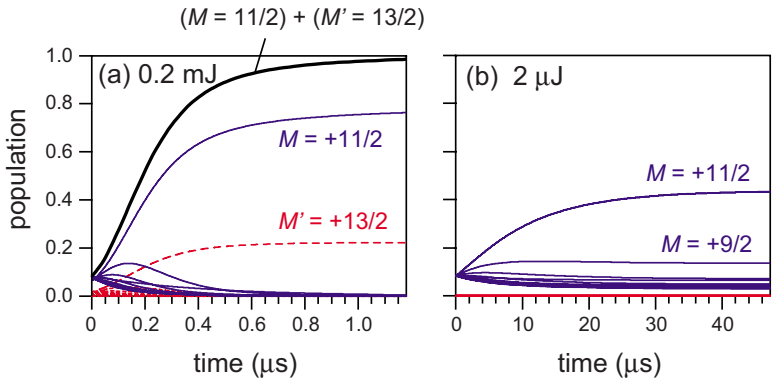

FIG. 4. (Color online) Numerical simulations of the populations in the magnetic sublevels, M ($F=11/2$) and M' ($F'=13/2$), as a function of time. The pulse energies of the incident σ^+ light are (a) 0.2 mJ and (b) 2 μJ. The lifetime of the laser pulse in the cavity is adjusted at 10 μs. Curves for the lower M and M' sublevels are not labeled [see the diagram in Fig. 3(b)].

5-ns laser pulse is too short to complete the spin polarization; the pulse stretching by the cavity plays a key role for optical pumping. On the other hand, Fig. 4(b) shows a very slow population change in the condition of $E=2$ μJ because of the low optical absorption rate; high-degree spin polarization is never achieved within the lifetime of the laser pulse. These are consistent with the results of the experiment; spin polarization was observed at 0.2 mJ [Fig. 2(c)], whereas there was no indication at 2 μJ [Fig. 2(d)].

In summary, we have shown that spin polarization of Mn^+ ions stored in an ion trap is achieved with an ultraviolet laser pulse by the cavity-assisted mechanism of optical pumping. The spin polarization in the $|F=11/2, M=+11/2\rangle$ sublevel was evidenced by dramatic changes in the absorption spectra measured subsequently to the optical pumping. The analysis of the enhanced peak in the $^7P_4 \leftarrow {}^7S_3$ absorption spectrum revealed the degree of spin polarization to be greater than $49\% \pm 6\%$ as a result of population transfer from the lower to the highest F level; the nuclear spin is polarized as well. A large number (about 10^8) of spin-polarized ions created in an ion trap would have applications as a spin-polarized ion source or target, e.g., an oriented collision partner in nuclear physics. We note that the present technique of optical pumping is applicable not only to dilute gases and ions, for which the multiple pass inside the cavity is advantageous, but also to optically thick targets, which may be placed behind the cavity and employ an elongated output pulse from the cavity as a pumping light.

We thank Kazuyuki Etou of Japan Aviation Electronics Industry, Ltd., for coating the high-reflectivity mirrors and Dr. Yukari Matsuo for valuable advice. The present study is supported by the Special Cluster Research Project of Genesis Research Institute, Inc.

[1] W. Happer, Rev. Mod. Phys. **44**, 169 (1972).
[2] A. Kastler, J. Phys. Radium **11**, 255 (1950).
[3] L. C. Balling, Adv. Quantum Electron. **3**, 1 (1975).
[4] D. J. Wineland *et al.*, Ann. Phys. **10**, 737 (1985).
[5] R. J. Knize, Z. Wu, and W. Happer, Adv. At. Mol. Phys. **24**, 223 (1988).
[6] J. Brossel and F. Bitter, Phys. Rev. **86**, 308 (1952).
[7] W. Demtröder, *Laser Spectroscopy: Basic Concepts and Instrumentation* (Springer, Berlin, 2002).
[8] G. T. Walker and W. Happer, Rev. Mod. Phys. **69**, 629 (1997).
[9] D. J. Wineland *et al.*, J. Res. Natl. Inst. Stand. Technol. **103**, 259 (1998).
[10] D. Budker and M. Romalis, Nat. Phys. **3**, 227 (2007), and references therein.
[11] T. Nakajima and N. Yonekura, J. Chem. Phys. **117**, 2112 (2002); T. Nakajima *et al.*, Appl. Phys. Lett. **83**, 2103 (2003); T. Nakajima, *ibid.* **88**, 111105 (2006).
[12] A. Terasaki, T. Majima, and T. Kondow, J. Chem. Phys. **127**, 231101 (2007).
[13] R. Kling and U. Griesmann, Astrophys. J. **531**, 1173 (2000).
[14] R. Kling, R. Schnabel, and U. Griesmann, Astrophys. J. Suppl. Ser. **134**, 173 (2001).
[15] R. J. Blackwell-Whitehead *et al.*, Mon. Not. R. Astron. Soc. **364**, 705 (2005).
[16] R. Engeln *et al.*, J. Chem. Phys. **107**, 4458 (1997).
[17] G. Berden, R. Engeln, P. C. M. Christianen, J. C. Maan, and G. Meijer, Phys. Rev. A **58**, 3114 (1998).
[18] A. O'Keefe and D. A. G. Deacon, Rev. Sci. Instrum. **59**, 2544 (1988).
[19] A. Terasaki, T. Kondow, and K. Egashira, J. Opt. Soc. Am. B **22**, 675 (2005).
[20] K. Egashira, A. Terasaki, and T. Kondow, J. Chem. Phys. **126**, 221102 (2007).
[21] E. U. Condon and G. H. Shortley, *The Theory of Atomic Spectra* (Cambridge University Press, London, 1935).
[22] The absorption line of $F'=13/2 \leftarrow F=11/2$ was so strong and narrow in the spectral width, compared with that of the incident laser pulse, that the profile of the signal laser pulse exhibited a biexponential-like decay [P. Zalicki and R. N. Zare, J. Chem. Phys. **102**, 2708 (1995)], where the decay rate of the fast component due to the absorbance of interest tends to be underestimated in the fitting procedure because of the slow component due to unabsorbed spectral portions.
[23] I. V. Hertel and W. Stoll, J. Appl. Phys. **47**, 214 (1976).
[24] I. V. Hertel and W. Stoll, Adv. At. Mol. Phys. **13**, 113 (1978).
[25] J. J. McClelland, in *Atomic, Molecular, and Optical Physics: Atoms and Molecules*, edited by F. B. Dunning and R. G. Hulet (Academic, San Diego, 1995), p. 145.